Femtosecond Charge Transport in Polar Semiconductors

A. Leitenstorfer, S. Hunsche, J. Shah, M. C. Nuss, and W. H. Knox
Bell Laboratories, Lucent Technologies, 101 Crawfords Corner Road, Holmdel, New Jersey 07733
(Received 7 December 1998)

The transient current response of bulk GaAs and InP is investigated at ultrahigh electric fields. On ultrashort time scales, the electronic system is far from equilibrium and overshoot velocities as high as 8×10^7 cm/s are observed. Our studies also lead to a detailed understanding of the ionic response of polar semiconductors. For the first time, carrier motion is determined with a resolution of 20 fs at fields up to 130 kV/cm. The dependence of the ultrafast dynamics on material and electric field provides new insights into the microscopic mechanisms governing nonequilibrium transport. [S0031-9007(99)09427-2]

PACS numbers: 78.47.+p, 42.65.Re, 72.15.Lh, 72.20.Ht

The ultrafast transport response of polar semiconductors biased at high electric fields is of fundamental interest in the physics of semiconductors. In recent years, numerous purely optical investigations have monitored the femtosecond dynamics of carrier energy distributions [1]. However, only a few studies of ultrafast high-field transport have been reported [2–5]. Furthermore, the transport experiments have primarily focused on the carrier acceleration and largely ignored the effects of the ionic lattice.

In this Letter, we present the first direct measurement of the femtosecond dynamics of high-field transport of carriers and ions in GaAs and InP crystals under conditions of extreme nonequilibrium. This goal is accomplished via direct detection of the amplitude and phase of the infrared radiation emitted by accelerating charges. We find that the polar crystal lattice contributes significantly to the current transients on femtosecond time scales, in contrast to the usual assumption that only the electronic part is important. We can isolate the contributions of carriers and the lattice, and determine the transient acceleration and velocity of carriers with a time resolution in the order of 10 fs. The maximum velocity overshoots and traveling distances during the nonequilibrium regime are directly measured for the first time. These observations allow us to determine the influence of various scattering processes on the dynamics of electron transport. Distinct differences are seen between GaAs and InP and interpreted in terms of the different band structures and coupling strengths of these important materials.

The basic idea of our experiment is to exploit the electromagnetic radiation emitted by an accelerating charge as a probe for ultrafast transport in semiconductors: Electron-hole pairs are generated near the fundamental gap in a *p-i-n* diode [6]. We work with 12 fs laser pulses of a central photon energy of 1.49 eV and a bandwidth of 120 meV. An electric field is applied over the intrinsic region by biasing the diode. The ultrafast separation of the photogenerated electrons and holes under the influence of the electric field creates a sheet of accelerating charges. In the far field, the amplitude of the THz radiation emitted by each dipole is proportional to the time derivative of the current, determined by three processes: (i) the femtosecond acceleration of free carriers in the electric field and their deceleration due to carrier-phonon scattering, (ii) the collective response of the polar crystal lattice reacting to the rapid change in the internal electric field caused by the motion of free carriers, and (iii) a current drop as the carriers leave the intrinsic zone within a few ps.

The excitation beam is made convergent by an off-axis parabolic mirror and hits the sample 12 mm before the confocal region under a grazing angle of incidence of 70°. The spot size on the large-area *p-i-n* diode is 3 mm by 1 mm. In this way, carrier densities can be kept low around 5×10^{14} cm^{-3} to avoid field screening, carrier-carrier scattering, and optical rectification. The THz signal is monitored at the position of the focus of the reflected pump light. This special geometry ensures that all excited elementary dipoles add up constructively in the sampling point and the resulting THz transient is identical to the radiation emitted by a single electron-hole pair. All experiments are performed at room temperature.

We apply ultrabroadband electro-optic sampling [7,8] to detect the bremsstrahlung. The electric field of the THz transients induces birefringence in an electro-optic crystal and the difference in refractive index is probed by a time delayed laser pulse which is coupled collinearly into the THz beam via a 500-μm Si filter coated with 4 nm of Au. Our data are obtained with two different detectors: $\langle 110 \rangle$ oriented ZnTe and GaP with a thickness of approximately 8 and 13 μm, respectively. After the sensor, the probe beam is transmitted through a quarter wave plate and split by a Wollaston prism [7]. The normalized differential signal $\Delta I/I$ between the polarization components of the probe is proportional to the momentary THz electric field present in the electro-optic crystal. $\Delta I/I$ is analyzed by shot-noise limited differential detection with a relative sensitivity of 10^{-8} Hz$^{-1/2}$. The spectral bandwidth of our system approaches 70 THz [8].

Figure 1 depicts the THz signals for GaAs and InP at various dc electric fields, as measured with the ZnTe detector. These transients reflect the time dependence of the free carrier and ionic charge acceleration as discussed

 0031-9007/99/82(25)/5140(4)$15.00 © 1999 The American Physical Society

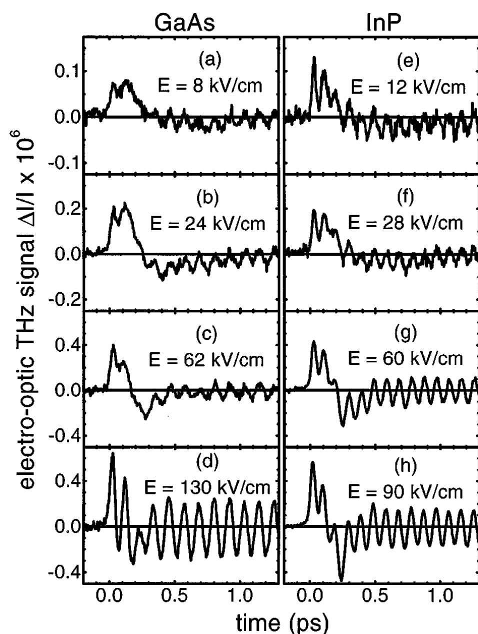

FIG. 1. THz transients from GaAs [(a)–(d)] and InP [(e)–(h)] p-i-n diodes for different bias fields E and at 300 K. Note the different scales of the abscissa.

above. The free carrier part of the data is dominated by the dynamics in the conduction band due to the low effective mass of the free electrons: For electric fields E below or close to the Gunn threshold, i.e., 4 kV/cm in GaAs and 12 kV/cm in InP, the momentum relaxation by polar-optical scattering confines most of the electrons to the Γ valley. In both materials, an acceleration period lasting approximately 350 fs is indicated by the positive THz field [Figs. 1(a) and 1(e)]. The small negative amplitude at later times is caused by the decrease of current related to carriers leaving the intrinsic region of the p-i-n diode. In addition to the radiation of the free carriers, the signals also demonstrate the oscillation of the ions in the polar crystal lattice: The polarization originating from the displacement of the electron-hole pairs leads to a small but ultrafast change of the internal electric field. The polar crystal lattice becomes excited impulsively since the ions accelerate towards their new equilibrium positions [9]. As a result, a component oscillating with the LO phonon frequency (8.8 THz in GaAs and 10.3 THz in InP) is superimposed on the signal originating from free carrier transport. These oscillations decay with time constants in the order of 5 ps, reflecting the LO phonon dephasing via anharmonic interactions.

When the bias field is increased to 24 kV/cm in GaAs [Fig. 1(b)], the situation changes distinctly and a strong negative signal indicating a fast *deceleration of charges* appears between 250 and 700 fs: The momentum gain from the field is now much stronger than the polar-optical momentum loss and the electrons reach average velocities substantially above the equilibrium drift (velocity overshoot). The subsequent transfer into the L and X valleys of the conduction band (Γ to L splitting in GaAs: 330 meV) leads to a reduction in mobility and a fast deceleration. Consistent with the stronger polar-optical scattering and higher intervalley threshold (approximately 600 meV) in InP, the negative signal connected to the overshoot phenomenon is much less developed at a comparable electric field [Fig. 1(f)]. When the field is increased to 60 kV/cm, the nonequilibrium features in both materials become faster [Figs. 1(c) and 1(g)]. Finally, at fields in the order of 100 kV/cm in GaAs, the initial acceleration-deceleration cycle of the electrons approaches the oscillation period of the zone center LO phonon (115 fs) and the energy content of the radiation emitted at the LO frequency becomes very prominent [Fig. 1(d)]. These resonant conditions are not yet reached in InP at 90 kV/cm [Fig. 1(h)] since the larger Γ-L splitting results in a longer acceleration regime for the electrons while the LO cycle is slightly shorter in this compound (98 fs).

In Fig. 2, the THz signals from the GaAs sample are presented on an expanded time scale. Here, the transients have been corrected for the response of the GaP detector [8]. These data allow a precise determination of the time it takes to reach the maximum velocity in the p-i-n structure: This value is given by the first zero crossing of the corrected THz transients (marked with arrows) which corresponds to zero average acceleration. The maximum velocity is measured to occur after 200 and 120 fs at bias fields of 30 and 62 kV/cm, respectively. These findings are in good agreement with Monte Carlo simulations modeling ultrafast transport of photocarriers [10]. To our knowledge, the measurements represent the first direct confirmation for the correctness of a semiclassical description of transport on a time scale of 10 fs. The experiments also provide information at higher fields where no theoretical calculations are presently available in the literature. We find the highest drift velocity to occur after an acceleration regime as short as 55 fs at 130 kV/cm. Based on the assumption of ballistic transport within the Γ valley in such a high field, we calculate a lower time limit of 40 fs for the electrons to gain the energy necessary for intervalley scattering. Since the velocity peaks already 55 fs after excitation, we estimate an extremely short value of 20 fs for the effective transfer time into the side minima.

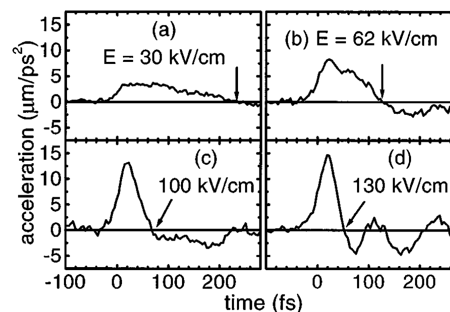

FIG. 2. (a)–(d): Early time regime of charge acceleration in GaAs at different electric fields E. The temporal positions corresponding to the maximum current are marked with arrows.

The interplay between electronic and ionic contributions to the femtosecond charge acceleration is demonstrated in Fig. 3. In Fig. 3(a), the original THz signal from the InP emitter at a bias field of 90 kV/cm is shown. This transient has been corrected for the response of the ZnTe electro-optic sensor [8]. The THz electric field $E_{\mathrm{THz}}(t)$ is proportional to the second time derivative of the free carrier displacement $D(t)$ minus the lattice polarization $P(t)$:

$$E_{\mathrm{THz}}(t) \propto \frac{\partial^2}{\partial t^2}[D(t) - P(t)]. \quad (1)$$

In the frequency domain, $D(\omega)$ and $P(\omega)$ are connected via the frequency dependent linear dielectric function $\varepsilon(\omega)$ [11]:

$$P(\omega) = [1 - \varepsilon(\omega)^{-1}] \times D(\omega). \quad (2)$$

Thus, the spectrum of the electromagnetic transients results from the free-carrier displacement renormalized by $\varepsilon(\omega)^{-1}$:

$$E_{\mathrm{THz}}(\omega) \propto \omega^2 \times \frac{D(\omega)}{\varepsilon(\omega)}. \quad (3)$$

The influence of the polar lattice is clearly visible in the Fourier transform of the THz transient [Figs. 3(b) and 3(c)]: The amplitude spectrum is sharply peaked at the LO phonon frequency of InP because the real part of the dielectric function goes to zero. Consequently, any electric disturbance around ν_{LO} is strongly enhanced [Eq. (3)]. In contrast, a minimum is found at the TO phonon resonance since $|\varepsilon(\omega)|$ has a maximum at ν_{TO}. A phase shift of π occurs between ν_{TO} and ν_{LO}. It is connected to the retarded response of the ion lattice. In a narrow band around ν_{TO}, our data contain no physical information since the values fall below the noise level.

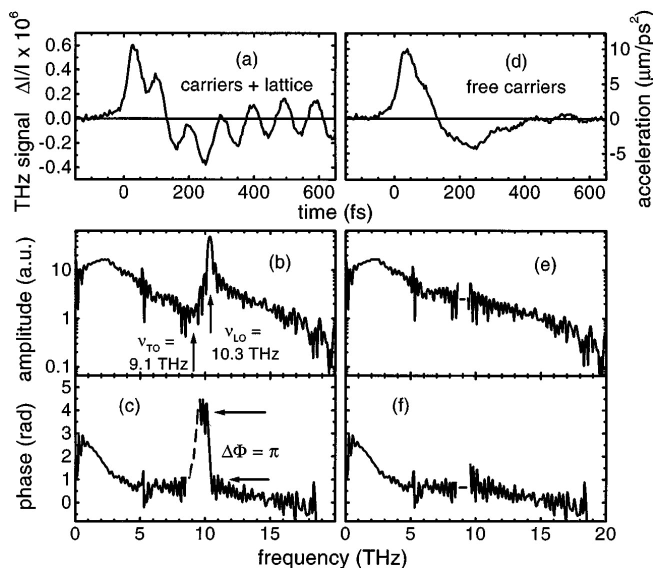

FIG. 3. (a)–(c): Time trace, amplitude, and phase spectrum for the overall current change (including the polar lattice) in InP at a bias field of 90 kV/cm. (d)–(f): Free carrier contribution to the signals after correcting for the linear dielectric function.

The free carrier contribution to the THz emission is obtained by correcting the amplitude and phase spectra of the original signal with the dielectric function of InP [12], according to Eq. (3). The results are seen in Figs. 3(e) and 3(f): We get a continuous rolloff of the amplitude between 2 and 20 THz and the phase shift at the LO frequency is removed. The inverse Fourier transform of the corrected spectra represents the relative acceleration of electrons and holes in the time domain [Fig. 3(d)].

It has to be emphasized that our analysis of the radiation from coherent phonons is valid only in the limit of an extremely thin dipole layer (the intrinsic zone) on a conducting half space (the n^+ substrate) where the emission characteristics is frequency independent [13]. When free carriers are excited in the surface field of a dielectric half space [14,15], additional effects arise since the deformation of the dipole lobes strongly reduces THz emission into free space at frequencies with a large value of the dielectric function [13,15].

Our measurement allows us to obtain quantitative values of the electronic transport parameters as follows: Integrating the corrected THz transients twice in time yields a quantity that is proportional to the average carrier displacement. After a few ps, all carriers have left the i region of the diode, and the double integrals saturate at a constant value that can be equated with the known effective width of the high-field zone. In this way, a calibration factor is obtained for the time dependent carrier displacement and its derivatives, the average velocity and acceleration. As an example, the drift velocity is depicted versus time for InP at 90 kV/cm in Fig. 4(a). The transient velocity exhibits a distinct maximum originating from the velocity overshoot of the electrons in the Γ valley before they get scattered to the low-mobility side valleys. We note that the peak velocity of 8×10^7 cm/s is an order of magnitude higher than the equilibrium drift velocity of electrons of 0.8×10^7 cm/s [16]. The equilibrium drift velocity for holes at 90 kV/cm is approximately 1×10^7 cm/s [17]. Our results for the drift velocity after the initial nonthermal regime (e.g., after approximately 0.5 ps in Fig. 4) are in excellent agreement with the sum of the known electron and hole equilibrium velocities. The carrier displacement in InP at 90 kV/cm is shown in Fig. 4(b): A strongly nonlinear initial regime (I) is followed by equilibrium transport (II). After approximately 1.5 ps, the displacement starts to

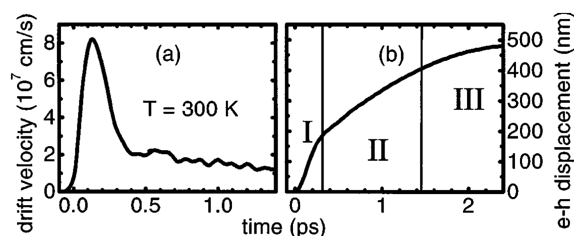

FIG. 4. Drift velocity (a) and electron-hole displacement (b) versus time in InP at 90 kV/cm.

level off because the amount of carriers having left the drift region becomes significant (III).

We can also estimate the coherent displacement of the atoms quantitatively, taking into account the effective charge of the unit cell and the density ratio between free electrons and lattice sites. Surprisingly, it turns out that the maximum amplitude of the relative vibration of the ions in InP at 90 kV/cm is 10^{-16} m, i.e., approximately 7 orders of magnitude smaller than the lattice constant. This finding demonstrates a unique sensitivity of our measurements for nuclear motion.

In Fig. 5(a), the maximum drift velocities are depicted versus electric field: Above 50 kV/cm, the values are higher in InP due to its larger intervalley threshold energy as compared to GaAs. Figure 5(b) displays the electron-hole displacement reached at the point of maximum drift velocity as a function of electric field. For comparison, the calculated distance necessary for an electron to gain an energy equivalent to the Γ-L splitting is presented for GaAs (dashed line) and InP (full line): In the limit of weak scattering within the Γ valley, the maximum velocity is expected to occur after a transit length close to the distance it takes for the electrons to reach the intervalley threshold. This picture is found to be valid at high fields. In this regime, the nonequilibrium transport of electrons is influenced only by the efficient momentum redistribution due to interaction with intervalley phonons via the deformation potential.

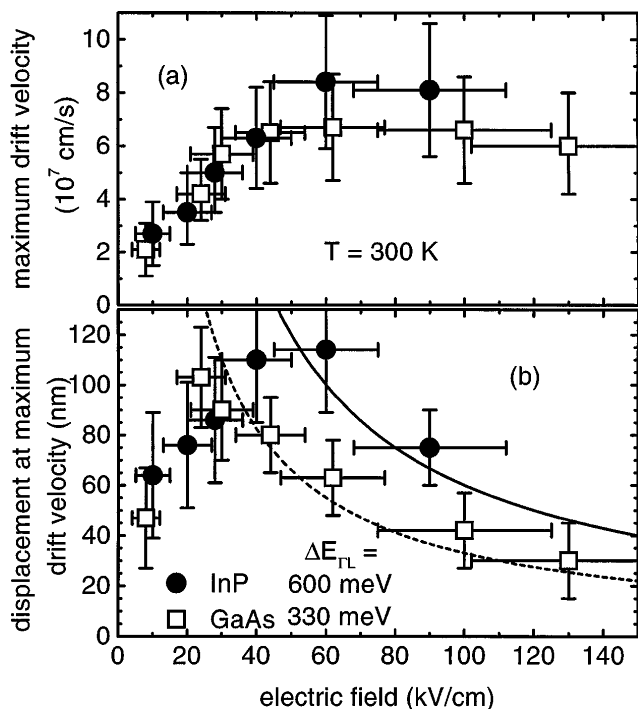

FIG. 5. (a) Maximum drift velocity and (b) carrier displacement reached at the point of maximum drift velocity versus electric field. The calculated drift distances to gain a field energy corresponding to the intervalley threshold $\Delta E_{\Gamma L}$ are depicted for GaAs (dashed line) and InP (solid line), respectively.

In conclusion, we have directly investigated femtosecond transport in polar semiconductors under high electric fields in a regime where the free carriers are far from equilibrium. The current response in GaAs and InP is studied with a temporal resolution of 20 fs and in a previously unexplored regime of electric fields of up to 130 kV/cm using a powerful experimental technique. The measurements provide direct insight into the influence of different scattering processes and band structure effects on the ultrafast electronic conduction in these materials. Coherent excitation of the crystal lattice is found to contribute significantly to the charge acceleration on ultrashort time scales. The ionic part of the measured current change emerges from the coupling between free carrier displacement and lattice polarizability via the linear dielectric function of the polar materials.

We wish to thank J.E. Cunningham, T.C. Damen, K.W. Goossen, E.P. Ippen, W.Y. Jan, W. Kaiser, D.M. Tennant, and G. Zhang for valuable contributions. This work was partially supported by the NEDO Femtosecond Technology Project.

[1] For an overview, see J. Shah, *Ultrafast Spectroscopy of Semiconductors and Semiconductor Nanostructures* (Springer, Berlin, 1996).
[2] W. Sha, J.-K. Rhee, T.B. Norris, and W.J. Schaff, IEEE J. Quantum Electron. **28**, 2445 (1992).
[3] H. Heesel *et al.*, Phys. Rev. B **47**, 16 000 (1993).
[4] B.B. Hu *et al.*, Phys. Rev. Lett. **74**, 1689 (1995).
[5] P. Uhd Jepsen, R.H. Jacobsen, and S.R. Keiding, J. Opt. Soc. Am. B **13**, 2424 (1996).
[6] The diodes consist of a 5 nm semitransparent Ti top contact, a 20 nm p^+ region, and a 500 nm high-purity intrinsic zone MBE grown on n^+ substrates.
[7] Q. Wu and X.-C. Zhang, Appl. Phys. Lett. **71**, 1285 (1997).
[8] A. Leitenstorfer, S. Hunsche, J. Shah, M.C. Nuss, and W.H. Knox, Appl. Phys. Lett. **74**, 1516 (1999).
[9] G.C. Cho *et al.*, Phys. Rev. Lett. **65**, 764 (1990); T.K. Cheng *et al.*, Appl. Phys. Lett. **57**, 1004 (1990).
[10] G.M. Wysin, D.L. Smith, and A. Redondo, Phys. Rev. B **38**, 12 514 (1988).
[11] Equation (2) is obtained from the definitions for the displacement, $D = \varepsilon_0 E + P$, and for the dielectric function, $D = \varepsilon\varepsilon_0 E$, via elimination of the electric field E. See, e.g., J.D. Jackson, *Classical Electrodynamics* (Wiley, New York, 1999), 3rd ed., pp. 153, 296, 309. Note that in order to be consistent with our treatment, the ε used in this reference has to be replaced by $\varepsilon\varepsilon_0$.
[12] *Handbook of the Optical Constants of Solids,* edited by E. Palik (Academic Press, New York, 1985).
[13] W. Lukosz, J. Opt. Soc. Am. **71**, 744 (1981).
[14] T. Dekorsy *et al.*, Phys. Rev. Lett. **74**, 738 (1995).
[15] M. Tani *et al.*, J. Appl. Phys. **83**, 2473 (1998).
[16] T.H. Windhorn, L.W. Cook, M.A. Haase, and G.E. Stillman, Appl. Phys. Lett. **42**, 725 (1983).
[17] V.L. Dalal *et al.*, J. Appl. Phys. **42**, 2864 (1971).